

## ANALYSIS OF A SWIMMERS HAND AND ARM IN STEADY FLOW CONDITIONS USING COMPUTATIONAL FLUID DYNAMICS

Barry Bixler<sup>1</sup> and Scott Riewald<sup>2</sup>

<sup>1</sup>Honeywell Engines & Systems, Phoenix, AZ; <sup>2</sup>USA Swimming, Colorado Springs, CO.

As an alternative to the experimental determination of the hand and arm propulsive forces generated by swimmers, the numerical technique of computational fluid dynamics (CFD) has been used to calculate the steady flow around a swimmer's hand and arm at various angles of attack. Significant boundary layer separation was seen, ruling out the use of Bernoulli's equation to mathematically describe the lift generated by a swimmer. Computation of 3D lift is necessary to describe the propulsion generated by the arm at all angles of attack and the hand near angles of attack of 90 degrees. Force coefficients computed for the hand and arm compared well with steady-state coefficients determined experimentally. Such comparisons validate the chosen CFD techniques, and are an important first step toward the use of CFD for determining swimming hydrodynamic forces in more realistic unsteady flow conditions,

**KEY WORDS:** drag, lift, computational fluid dynamics, swimming, hand, arm

**INTRODUCTION:** Swimming propulsion is a phenomenon not fully understood, and to date, the research on propulsion has been strictly experimental. Wood (1977) used a wind tunnel to determine the force coefficients of a hand and forearm, but the lift forces were strictly 2D and the third dimension was neglected. Schleihauf (1979) also developed 2D lift forces when flume-testing a hand model. Interference drag was approximately accounted for when it was assumed the support rod encountered equal drag force with or without the hand attached. Berger, de Groot, and Hollander (1995) measured force coefficients on a hand and arm using a tow tank. Lift calculations were 3D, but the model pierced the water free surface, resulting in wave and ventilation drag. Thayer (1990) and Sanders (1999) showed experimentally that unsteady flow can significantly affect hand drag.

These researchers revealed the difficulties involved in conducting such studies experimentally. They had to choose between unwanted wave and ventilation drag, or inaccurate interference drag. An alternative approach, previously unused for the evaluation of arm and hand swimming propulsion, is to apply the numerical technique of computational fluid dynamics (CFD) to calculate the solution. In addition to avoiding inaccurate drag, it can show detailed characteristics of fluid flow. This paper compares steady-state force coefficients calculated using CFD methods to those obtained experimentally. Such comparisons validate the chosen CFD techniques, and are an important first step toward the use of CFD for determining swimming hydrodynamic forces in unsteady flow conditions.

**METHODS:** A CFD model was created based upon an adult male's right forearm and hand with the forearm fully pronated. The thumb was adducted, and the wrist was in a neutral position. This geometry protruded into a dome-shaped mesh of fluid cells from its base (Fig 1). The model's origin and x-y plane were in the plane of the dome base, and the z axis extended from the origin through the distal end of the fourth finger. The x axis was defined by the vector extending from the distal end of the fourth finger to the distal end of the index finger, then projected onto the x-y plane. The CFD mesh contained 215,000 cells.

The angle between the model's x axis and the flow direction is called the angle of attack. Angles of attack between -15 and 195 degrees in maximum increments of 15 degrees were evaluated. Water velocity was steady and prescribed to the inlet portion of the dome surface. For all flow cases, the prescribed flow was parallel to x-y plane (zero sweepback angle). The skin roughness was smooth (shaved), accomplished by setting the roughness height equal to zero. Density and viscosity values were chosen for water at 22.6 degrees C and the water velocity was varied between 0.3 and 4.0 m/s. The dome's base was a plane of symmetry, requiring the flow there to remain in that plane.

CFD techniques replace the Navier-Stokes fluid flow equations with discretized algebraic expressions that can be solved by iterative computerized calculations. The Fluent CFD code (Fluent Inc., Lebanon, NH) was used develop and solve these equations. The flow was assumed to be incompressible. All numerical schemes were second order, and non-equilibrium wall functions were used for boundary layer flow. The standard k- $\epsilon$  turbulence model was applied for a turbulence intensity of 1% and a turbulence length of 0.1 m.

The independent variables were angle of attack and fluid velocity at the inlet boundary. The dependent variables were pressure and velocity of the fluid within the dome. Component forces were calculated by integration of the pressure on the hand/arm surfaces. Force coefficients were then calculated for the hand, arm, and hand/arm combined using:

$$C_i = \frac{F_i}{\frac{1}{2} \rho V^2 A}$$

Where:  $F_i$  are the drag, lift, and axial forces and  $C_i$  are the corresponding coefficients

$\rho$  is the fluid density

$V$  is the steady free stream velocity of the fluid relative to the hand and arm

$A$  is the maximum projected area of the hand, arm, or hand/arm combination.

Drag forces (parallel to the flow direction), 2D lift forces (perpendicular to the drag force and parallel to the x-y plane), and axial forces (in the z direction) were computed by the model. The 3D lift force is the square root sum of squares of the axial and 2D lift forces. Drag and 3D lift forces are always positive, but axial and 2D lift forces can be positive or negative.

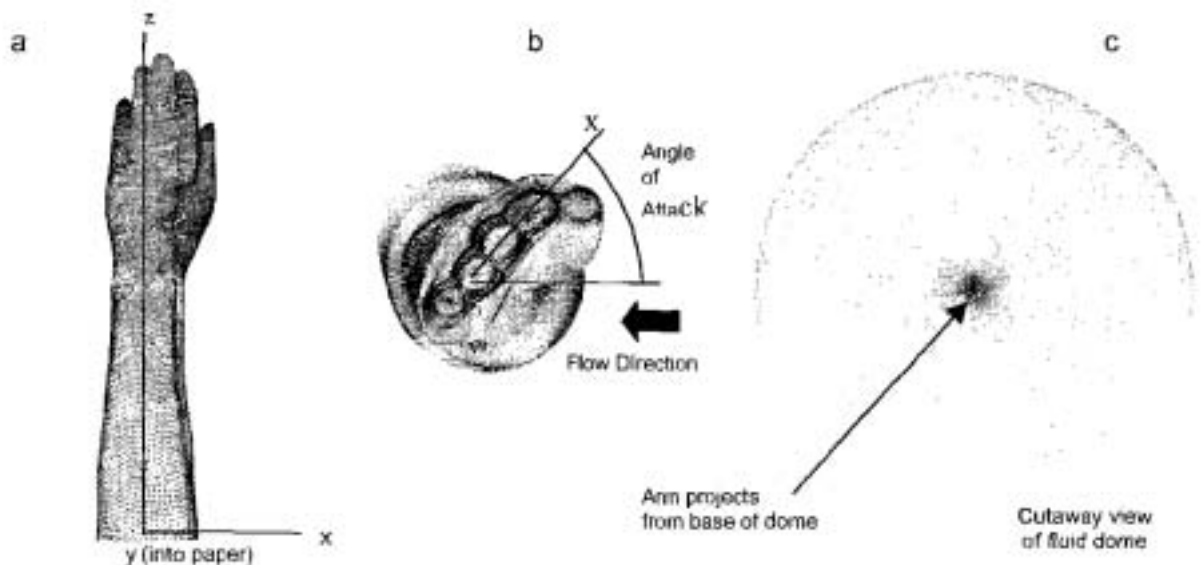


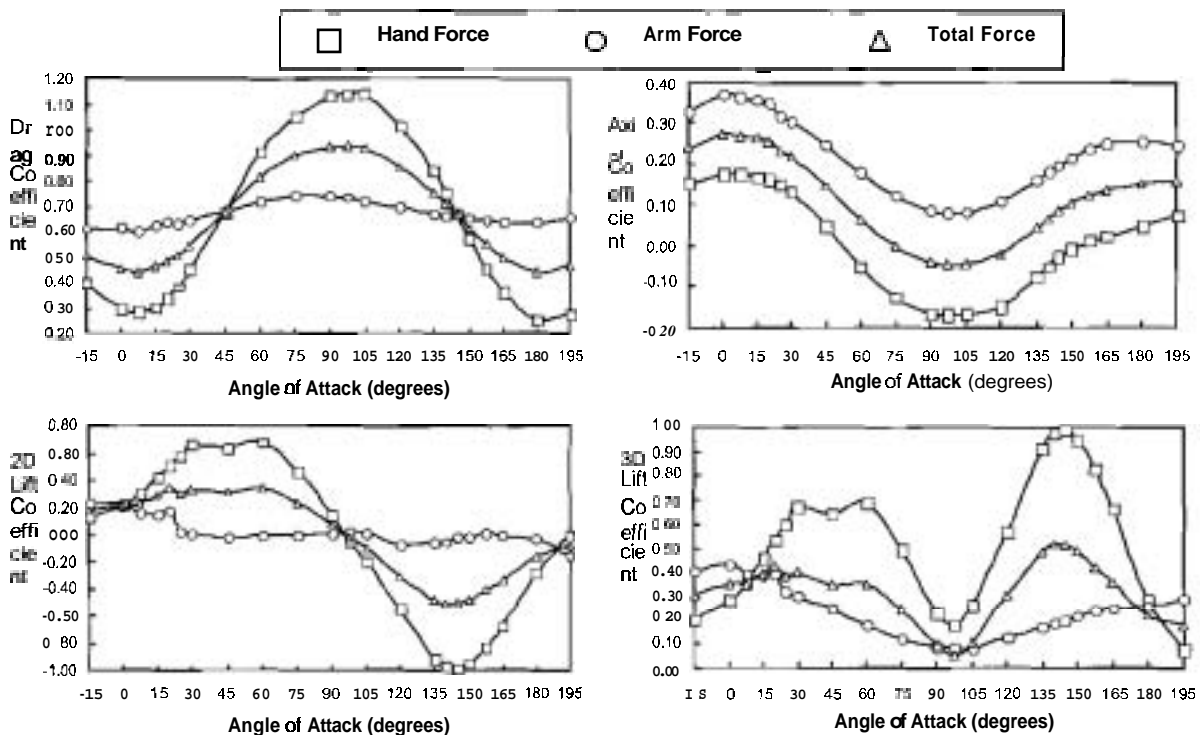
**Figure 1 - Figures 1 a -1c show the model (including the dome and hand-arm extending from its base) with the angle of attack and the global coordinate system defined.**

**RESULTS:** CFD Flow visualization is informative, and the oilfilm plot below clearly reveals significant boundary layer separation. Separation occurred at all attack angles, showing that Bernoulli's equation should not be used to explain the lift that swimmers can create.



Figure 2

Calculated force coefficients showed predictable trends. Arm drag was essentially constant ( $C_d = 0.65$ ), and arm lift was zero. Hand drag was minimum near angles of attack of 0 and 180 degrees and peaked at 95 degrees ( $C_d = 1.15$ ). Hand lift was zero at 95 degrees and peaked near 55 and 140 degrees, with more lift generated when the little finger leads than when the thumb leads. Axial coefficients were significant for the arm at all angles of attack and for the hand near angles of attack of 90 degrees, revealing that force component evaluations should be three-dimensional, rather than two-dimensional. All force coefficients were constant for velocities between 1.0 to 3.0 m/s (for a given angle of attack). Comparisons were made with experimentally measured data (see discussion).



**Figs 3a -3d: Force Coefficients vs. Angle of Attack for a Velocity of 2 m/sec with a zero degree sweepback angle and turbulence intensity of 1% and turbulence length of .1 m**

**DISCUSSION:** The steady-state force coefficients calculated using CFD methods were compared to steady-state coefficients obtained experimentally by Wood (1977), Schleihauf (1979), and Berger, de Groot, and Hollander (1995). Such comparisons are an important first step toward the use of CFD methods for determining swimming hydrodynamic forces in unsteady flow conditions. The zero degree angle of attack was defined differently in each experiment, and prior to comparison with CFD results, the differences in zero degree orientation were accounted for.

Wood (1977) tested a hand and half of a forearm in a wind tunnel, and the CFD drag and 2D lift coefficients (using only half of the forearm) compare very well with Wood's coefficients (Figure 4a). Schleihauf (1979) modeled a hand alone in a flume, and the CFD results are compared to the flume results using the force sign convention of the CFD model (Figure 4b). Although the comparison is satisfactory, the flume drag coefficients are consistently slightly higher than the CFD drag coefficients. A likely reason is flume turbulence, which increases lift and especially drag. There was also a local divergence of the CFD and experimental results near an angle of attack of 15 degrees, where the flume lift coefficient showed a localized peak. This occurrence could be caused by a partial abduction of the thumb in the flume model, where the thumb acts as the forward slat does in a slotted airplane wing.

This same local lift force peak was seen in a study by Berger et al (1995). Comparisons with CFD, now using total surface area as the reference area, are good for the hand alone (Figure 4c), but less favorable for the hand/arm combination (Figure 4d). The larger towing tank coefficients could be the result of wave and ventilation drag caused by the arm piercing the free water surface. Deformation of the free surface of the water accompanies such drag, and may be the reason Berger et al. found the axial forces ( $F_z$ ) to be small.

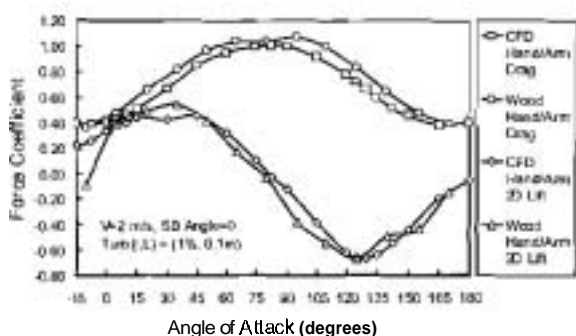


Fig 4a Comparison of Hand/Arm Force Coefficients for CFD and Wood (based upon maximum projected area)

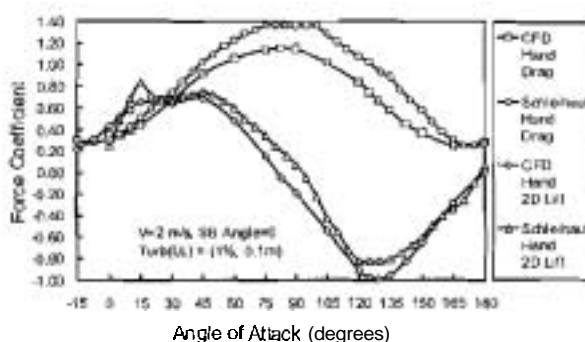


Fig 4b Comparison of Hand Force Coefficients from CFD and Schleihauf (based upon maximum projected area)

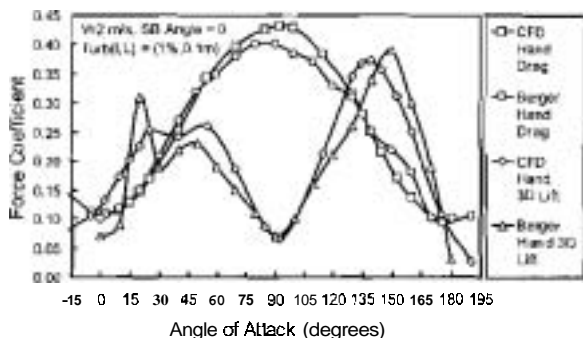


Fig. 4c Comparison of Hand Face Coefficients from CFD and Berger et al. (model 2) (based upon total surface area)

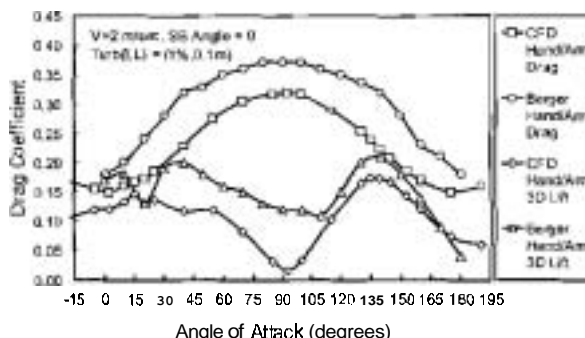


Fig. 4d Comparison of Hand/Arm Force Coefficients for CFD and Berger et al. (model 2) (based upon total surface area)

Figures 4a – 4d - Comparison of CFD force coefficients to experiment

**CONCLUSION:** The present study serves to establish CFD methodology as a technically viable and less expensive alternative to experimental testing of swimming propulsion. Our results compare favorably to the steady-flow data collected experimentally. In the future, the hand and arm model could be used to evaluate various aspects of unsteady motion, such as accelerations, decelerations, and multi-axis rotations. The ultimate goal of dynamically evaluating complete arm strokes and "designing" the optimal pulling pattern, will provide coaches with valuable stroke information that can be applied by their swimmers.

**REFERENCES :**

- Berger, M.A., de Groot, G., and Hollander, A.P. (1995) Hydrodynamic drag and lift forces on human hand/arm models. *Journal of Biomechanics*. 2, 125-133.
- Sanders, R.H. (1999) Hydrodynamic characteristics of a swimmer's hand. *Journal of Applied Biomechanics*, **15**, 3-26.
- Schleihauf, R.E. (1979) A hydrodynamic analysis of swimming propulsion, *Swimming 111*, International Series on Sports Sciences, (Volume 8, pp. 70-117). Baltimore: University Park Press.
- Thayer, A.M. (1990) Hand pressures as predictors of resultant and propulsive hand forces in Swimming. *Ph.D. Dissertation*. Iowa City, Iowa: University of Iowa.
- Wood, T.C. (1977) A fluid dynamic analysis of the propulsive potential of the hand and forearm in swimming. Master of Science Thesis. Halifax, Nova Scotia: Dalhousie University.